GRID-FORMING CONVERTERS – INEVITABILITY, CONTROL STRATEGIES AND CHALLENGES IN FUTURE GRIDS APPLICATION

Ali TAYYEBI
AIT and ETH Zürich – Austria
Ali.Tayyebi-Khameneh@ait.ac.at

Florian DÖRFLER
ETH Zürich – Switzerland
Dorfler@ethz.ch

Friederich KUPZOG
Austrian Institute of Technology – Austria
Friederich.Kupzog@ait.ac.at

Zoran MILETIC
Austrian Institute of Technology – Austria
Zoran.Miletic@ait.ac.at

Wolfgang HRIBERNIK
Austrian Institute of Technology – Austria
Wolfgang.Hribernik@ait.ac.at

ABSTRACT

At the heart of the energy transition is the change in generation technology: from conventional generation based on synchronous machines towards renewable energy sources interfaced with power electronic converters. The accompanying loss of rotational inertia and of the robust synchronization mechanism provided by synchronous machines and their controls is a challenge to the operation, control, and stability of the electric power system. In a future low-inertia power system, these functionalities have to be provided by proper control of so-called grid-forming power converters. This article provides a comprehensive review, a classification, and a critical comparison of different grid-forming converter control strategies in a simulation case study.

Key words *— Grid-Forming Converter, Synchronous Generator, Droop Control, Matching Approach, Synchronverter, Virtual Oscillator Control.*

INTRODUCTION

In line with recent technological developments increasing the feasibility of renewable energies utilization, one can expect a global transition towards a nearly 100% renewable grid [1]. As a result of massive integration of renewables, we witness a change in generation technology from fossil-fuel based power plants to renewable energy generation. Since renewables generate DC or variable AC output power (e.g., photovoltaics, variable frequency wind generators, etc.), power electronics-based solutions are the most viable energy conversion alternatives [2–4]. This sheds light on the possibility of integrating converters into the power system infrastructure replacing the synchronous generators (SGs). The absence of rotational inertia previously provided by SGs denatures the conventional power grid to a so-called *low-inertia system*.

The concept of a *grid-forming converter* (GFC) is fundamental to the operation of a low-inertia power system dominated by non-rotational generation. In such a scenario, grid-forming converters provide the reference for frequency and voltage and regulate these quantities. Furthermore, GFCs need to exhibit load-sharing, drooping and black start behaviors similar to SGs. Unlike SGs, GFCs do not induce any physical synchronization and stabilization mechanisms or provide any physical inertial response. These key features of SGs have to be realized via control of GFCs and separate energy storage elements. On the other hand, the fast response time of GFCs enables control at much faster time-scales than that of SG's primary control. Different control solutions replicating the SGs system-level functionalities (e.g., frequency/voltage drooping and/or inertial behavior) have been previously proposed in [5–8]; we refer to [9] and [10] for a review. Recently, also alternative promising grid-forming strategies rooted in nonlinear control methods have been proposed relying on matching and duality between power converters and synchronous machines [11–13] or the concept of controlling a converter as a nonlinear virtual limit cycle oscillator [14–17]. Furthermore, various measurement and communication based (i.e., IoT/ICT) solutions have been proposed [18],[19].

This paper aims to provide an updated review and a comparison of GFC control strategies. We classify the vast literature into five major GFC strategies, namely: 1) droop control, 2) synchronverter, 3) matching control, 4) virtual oscillator control (VOC) and 5) IoT/ICT based approaches. We provide a critical, un-biased, and fair comparison of the performance and robustness offered by these strategies by means of a system-level simulation case study. Finally, we list the challenges encountered and future problems to be solved for the different GFC strategies in low-inertia power systems.

REVIEW OF CONVERTER OPERATION AND MODELING

In this section, we present a few fundamental definitions regarding converter operational modes and GFC model configuration. With these preliminaries in place, we discuss GFC control strategies in Section 3.

Grid-Forming and Grid-Following Operation

Previous efforts to classify converter operation modes resulted in a handful of notions, but there is no universally accepted classification to date. Before embarking upon grid-forming control design, the definitions from [3] are presented here. *Grid-forming* mode refers to the DC/AC converter interaction with a non-stiff power grid or its operation in the complete absence of a power grid with SGs. Thus, GFC exhibits black start capability, frequency and voltage regulation, frequency-power droop and load sharing. Additionally, by transforming energy from a primary source, similar to the SGs, a grid-forming unit can dispatch required amount of power to the network loads. *Grid-following*

mode, on the other hand, highlights the applications in which the converter frequency is imposed by a stiff AC grid or another grid-forming unit. In this case, the network frequency/phase angle is extracted via a phase locked loop (PLL). Therefore, a grid-following unit locks onto the existing grid and injects (a possibly pre-defined amount of) active/reactive power in order to provide different services, e.g., primary control reserve, self-consumption, or voltage control.

Two-Level Voltage Source Converter Model

The two-level voltage source converter model in Figure 1 serves as a common implementation and comparison framework for various grid-forming control approaches. As shown in Figure 1, the converter's DC energy supply is modelled as a controllable current source i_{dc} in parallel with a resistance R_{dc} (resembling a Norton equivalent circuit) and DC link capacitance C_{dc}. The switching stage is represented by a full-bridge three-phase average model including DC/AC side current/voltage source depending on the modulating signal m_{abc}. This is cascaded by a three-phase star-connected filter composed of inductance L_f with series resistance R_f connected to the shunt capacitance C_f. The filter parameters are assumed to be identical for all the phases. In this setup, DC and AC side losses are modelled by R_{dc} and R_f, respectively. Furthermore, the DC link voltage v_{dc} and active power injection at the filter node p_m are measured for the GFC control implementations discussed below.

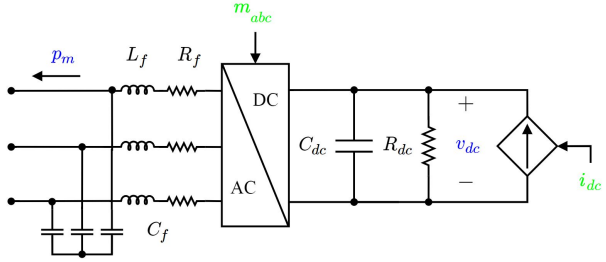

Figure 1. DC/AC converter circuit diagram.

EXISTING CONTROL STRATEGIES

In the sequel, we present a classification of the GFC control strategies into five major categories: 1) droop control, 2) virtual synchronous machine, 3) matching approach, 4) VOC and 5) ICT/IoT based approach. We particularly focus on the closely related first three categories and describe their control structure below. It must be noted that our focus is restricted to converter frequency control, which is the main mechanism that makes a converter grid-forming or grid-following. Thus, we merely control the switching node voltage amplitude to its set-point and disregard other voltage control concepts (such as a voltage droop as a function of active/reactive power) or voltage regulation at the filter node requiring additional inner tracking control loops. Finally, aside from frequency control, we consider the control of active power injection that enables us to look at set-point tracking and load sharing behavior.

Droop Control

The baseline solution to GFC control is to mimic the speed droop control of a synchronous machine. Droop control has initially been proposed in [5] as proportional control of active power and frequency, but many modified/improved versions have been reported [8]. Recalling the converter model in Figure 1, the corresponding active power and DC link voltage controllers are depicted in Figure 2 [9]. The proportional droop gain m_p trades off the deviation of the frequency ω from its set-point ω^* with the injected power p_m deviation from its set-point p^*. Furthermore, the constant AC voltage reference amplitude v_m^* is set such that switching node voltage is nominal when tracking p^*. Therefore, modulation signal m_{abc} is determined based on the phase angle and the reference AC voltage.

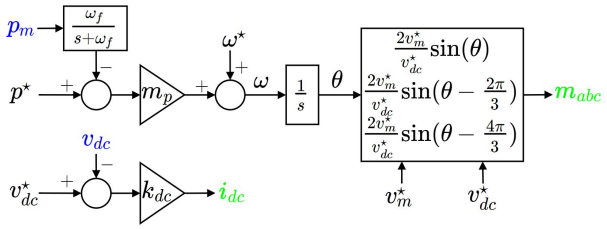

Figure 2. Droop control diagram.

Droop control can be further augmented with AC voltage and reactive power control loops with a cascade inner-outer loop design. An important implicit assumption behind droop control is the availability of a stiff DC voltage source. Hence, by choosing a high enough proportional gain k_{dc} which identifies i_{dc}, v_{dc} tracks v_{dc}^* at much faster time-scale than the internal frequency dynamics. Conversely, if the DC power supply is not sufficiently fast, then droop controllers have to be deliberately slowed down to ensure system stability For this reason and to avoid interaction with the AC grid line dynamics, the power measurements are usually low-pass filtered (with cut-off frequency ω_f) before being passed on to droop control [9],[16].

Virtual Synchronous Machine

A plethora of control strategies is inspired by virtually emulating the dynamics and control of a SG. The overarching paradigm is to control the converter terminal signals to behave like a SG. The various virtual machine implementations utilize a reduced-order and differential algebraic SG model and heavily rely on the converter AC side current/voltage/power measurement [6],[7],[9], and [10]. Consequently, the SG model encoded in a digital controller imposes an analogy between converter terminal and generator stator voltages. As an example of virtual SGs, the synchronverter control mechanism is shown in Figure 3 [6]. The AC voltage is set to the

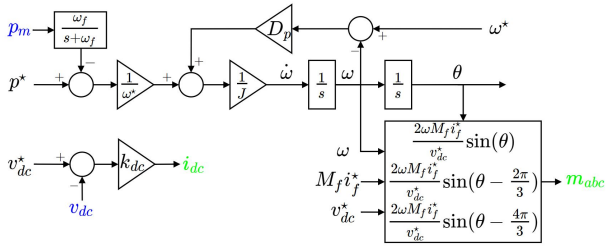

Figure 3. Synchronverter control diagram.

nominal value by an appropriate choice of a virtual excitation flux $M_f\ i_f^*$ (assumed to be constant). The generator mechanical swing equation is emulated with

the inertia constant J and the damping gain D_p. Note that the relation of frequency ω and active power p_m is the same as for droop control if D_p is chosen inversely proportional to the droop gain m_p in Figure 2, except that the synchronverter admits one more integrator accounting for the synthetic inertia. The implicit assumption for the synchronverter is similar to droop control: the DC voltage v_{dc} is controlled in a stiff fashion and on much faster time scales. Finally, similar to droop control the synchronverter can be augmented with further inner tracking controllers and outer regulation loops.

We briefly justify our choice of the synchronverter mechanism [6] over other emulation strategies. It has been observed that the emulation of a SG brings with it a few inherent challenges; see e.g., [2],[9],[10]. First, the post-fault response of a SG leads to large over-currents, which are unacceptable and undesired for a power converter. Second, the emulation of a detailed SG model is based on numerically integrating higher order nonlinear dynamics fed by (often filtered, averaged, and PLL-based) AC-side measurements which leads to a significant time delay in the grid-forming control loop. The synchronverter in Figure 3 is the *leanest* emulation concept (where all emulated dynamics are algebraic aside from the mechanical ones) for which the aforementioned disadvantageous effects are the least pronounced. Finally, we note the tuning recommendation $J<<D_p$ from [6], which (in the limit of vanishing virtual inertia over damping ratio $J/D_p=0$) effectively reduces the synchronverter control in Figure 3 to the droop control in Figure 2.

Matching Control

Based on the structural similarities between the SG and two-level power converter models different matching approaches are proposed in [11–13]. The dualities between the two models reveal a link between the converter DC link voltage and SG rotor angular frequency (similarly between the electro-static and kinetic energies stored in DC link and rotor respectively). We adopt the matching control from [11] illustrated in Figure 4. The core GFC control strategy relies on a measurement of the DC voltage v_{dc} only, which up to a constant factor η then induces the grid-frequency ω. Motivated by the analogy between generator torque and converter DC current, the primary DC energy source, the current source i_{dc}, regulates the frequency by controlling v_{dc}. Therefore, compared to previously mentioned methods DC side proportional control has a different interpretation. Furthermore, by changing i_{dc}, active power set-point tracking is achieved (similar to changing turbine mechanical torque). In this case, it is necessary to compensate the power losses in the DC and AC side of the converter. Lastly, AC side constant voltage amplitude is set in the same way as for the other control strategies.

At this point, we remark that matching control does not require any measurement of AC-side quantities: the modulation signal m_{abc} directly results from the DC voltage measurements. This appealing feature removes time delays encountered by processing AC measurements, and it unmasks the interactions between the converter AC side and the DC side (whereas the previous control strategies all implicitly require a time-scale separation of the AC-side grid-forming control and the stiff DC-side control).

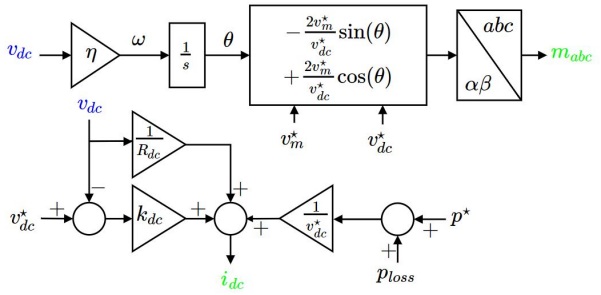

Figure 4. Matching control diagram.

VOC and IoT/ICT Based Approaches

In the following, we review two alternative GFC control strategies that are not directly (or indirectly) inspired by synchronous machines. Based on synchronization theory and methods from nonlinear control, [15] suggests a virtual oscillator based control (VOC) strategy. The VOC concept has been further refined and related to droop control in [14],[16], and a fully dispatchable version has been developed in [17]. Finally, aside from the previously mentioned GFC control strategies, a plethora of IoT/ICT approaches (based on ubiquitous sensing and communication) have been proposed [18],[19]. Due to inherent differences in their underlying assumptions and implementations (and our restricted focus on solely frequency and active power control without any AC voltage control) these two solutions are not investigated further in our comparison case study. We defer their review and detailed comparison to a future publication.

COMPARISON TEST CASE

In this section, we outline the results of a system-level simulation case study utilizing the standard IEEE 9-bus test system illustrated in Figure 5 in which the SGs are replaced by GFCs. System's base power, voltage, and frequency values are listed in Table 1.

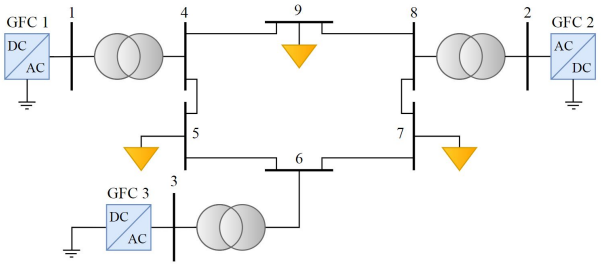

Figure 5. IEEE 9-bus test system.

In this case, three identically tuned GFCs (connected to bus 1, 2 and 3) are assumed to supply the network's resistive loads (connected at bus 5, 7 and 9 each 1 p.u.). The simulation case study in MATLAB/Simulink environment is repeated three times (i.e., by controlling all the GFCs via droop control, and similarly with the synchronverter and matching approaches). In order to provide an un-biased and fair comparison, the controllers are tuned to achieve the same steady-state frequency droop and power injections. Thus, for all three methods we allow the same frequency deviation when the active power demand deviates from the pre-defined GFCs set-points. Recalling the arguments in Section 3, and by

setting frequency deviation Δf droop control gain, synchronverter damping constant and matching DC side proportional gain are selected as

$$m_p = \frac{2\pi\Delta f}{S_b}\ ,\ D_p = \frac{1}{\omega^* m_p}\ ,\ k_{dc} = \frac{\eta}{v_{dc}^* m_p}\ ,$$

where S_b is the system base power and $\eta = \omega^* / v_{dc}{}^*$. The controllers parameters are presented in Table 1. Most importantly, as all the GFCs for each method are tuned identically, they all show identical proportional load sharing behavior. For instance, in droop control strategy if m_p is identical for all the GFCs, then

$$\frac{p_{m1} - p_1^*}{p_{m2} - p_2^*} = \frac{p_{m2} - p_2^*}{p_{m3} - p_3^*} = \frac{p_{m3} - p_3^*}{p_{m1} - p_1^*} = 1.$$

The simulation time in each case is 3 seconds including the following three scenarios: 1) For $t = 0$ we consider a black start to pre-defined set-points (1.2, 1 and 0.8 p.u. for GFC 1, 2 and 3, respectively) in a PLL free fashion (with all phase angles initialized at zero); 2) At $t = 1$ the load at bus 9 undergoes a step change from 1 to 1.5 p.u. (increasing the total network load from 3 to 3.5 p.u.) resulting in equal steady-state frequency deviation and, load sharing for all three methods. 3) Finally, at $t = 2$, we consider a loss of generation at bus 1. Hence, GFCs 2 and 3 take over the excess load while preserving load sharing and leading to higher frequency deviation. The frequency and active power time series are illustrated in Figure 6.

IEEE 9-bus test system base values					
S_b	100 MW	V_b	345 kV	f_b	50 Hz.
Converter model					
R_{dc}	0.1 Ω	C_{dc}	0.001 F	$v_{dc}^\star$	1035 kV.
R_f	0.1 Ω	L_f	500 μH	C_f	10 μF
Droop control					
Δf	0.3	m_p	1.885×10^{-8}	ω_f	$2\pi \times 5$
k_{dc}	1500	$v_m^\star$	281.69×10^3	$\omega^\star$	$2\pi \times 50$
Synchronverter					
D_p	168.87×10^3	J	5×10^3	ω_f	$2\pi \times 5$
k_{dc}	1500	$M_f i_f^\star$	897.5	$\omega^\star$	$2\pi \times 50$
Matching					
k_{dc}	0.0156	$v_m^\star$	281.69×10^3	η	3.035×10^{-4}

Table 1. Simulation case study parameters.

Notice that droop control results in undesired oscillations due to adverse interactions with the line dynamics. This transient oscillatory behavior can be improved by including appropriate filters for the measured power p_m. The synchronverter displays oscillatory behavior and overshoots due to the second-order (virtual) inertial dynamics. These effects are especially pronounced when

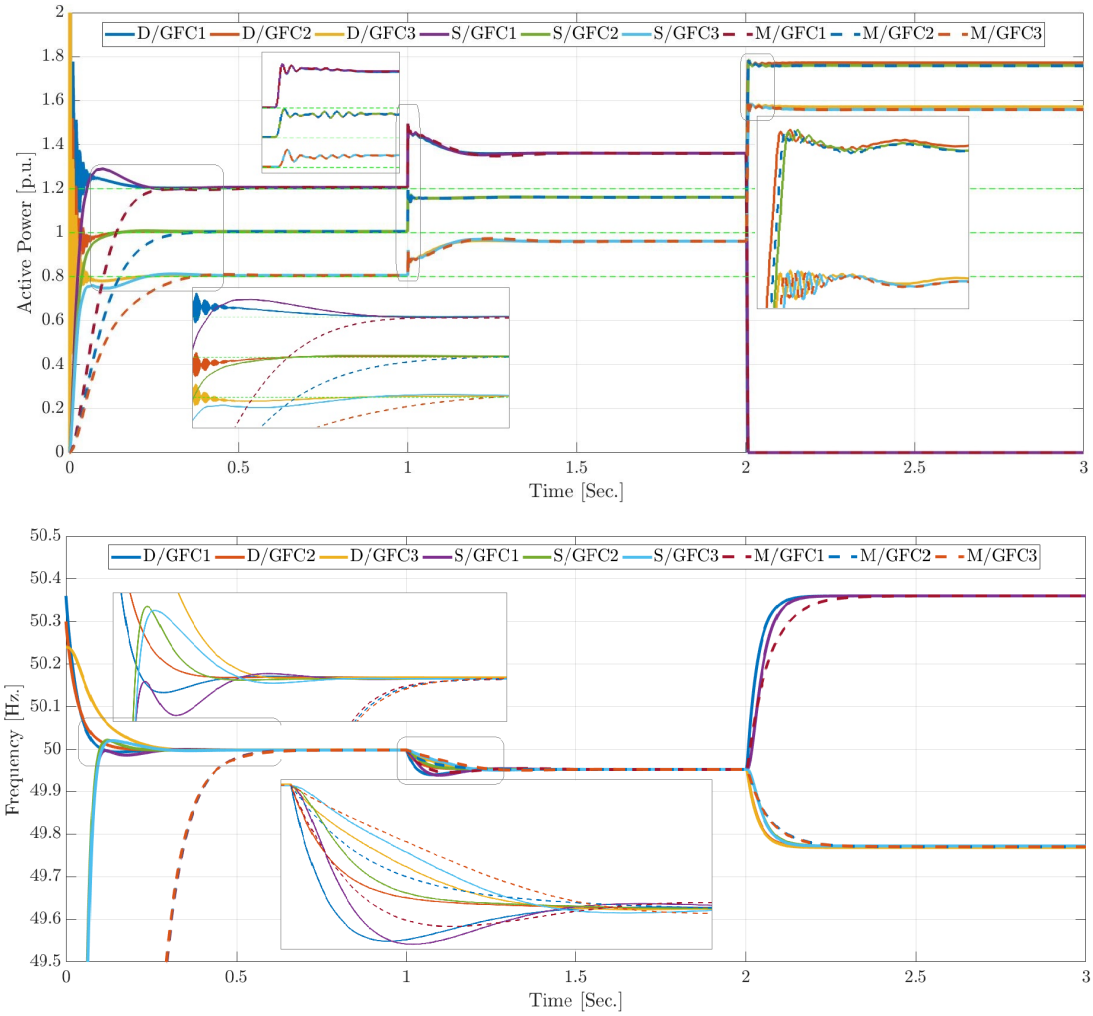

Figure 6. GFCs 1-3 active power (top) and frequency (bottom) plots. Droop control (D), Synchronverter (S), and Matching (M).

filtering the power measurements and for high Δf values. Note that the matching approach achieves a much smoother, albeit slower, transient behavior than the other methods. Its comparatively slow dynamics are related to the fact that the AC and DC regulation are inherently coupled, see Figure 4, and the AC variables are controlled via actuation on the DC side. On the contrary, the droop and synchronverter assume a stringent time-scale separation between AC and DC dynamics and become unstable otherwise. Filtering of active power has no impact on matching control. Finally, we remark that for low Δf values (and thus lower m_p and higher D_p and k_{dc}) the convergence speed of all three methods becomes comparable.

FURTHER CHALLENGES

As a closing argument on GFC control strategies, we list the critical challenges encountered and problems to be resolved for large-scale GFC application in future low-inertia grids. The main device-level challenges are: 1) counteracting the imperfect measurement (e.g., delay and noise), 2) choice and control of an adequate primary energy source and GFC compatibility with realistic DC energy sources (batteries, photovoltaics and wind generators), and 3) limiting the converter inrush current. Additionally, the system level key issues are: 1) stability/synchronization of interconnected systems of GFCs, 2) backward compatibility with SGs, 3) GFC response to transmission system topology change, and 3) optimal GFC sizing/allocation/planning. These challenges must be thoroughly investigated for GFCs in order to fully replace SGs in low-inertia systems. Moreover, further inner and outer control loops (e.g., for voltage and reactive power) must be integrated to the previously mentioned control structures – thus facilitating their comparison to VOC and ICT/IoT based strategies. Lastly, the case study simulations should be done in higher fidelity environment such as controller/power hardware in the loop.

SUMMARY AND CONCLUSIONS

In this paper, we presented an updated review on GFC control strategies followed by a classification of existing methods into five major categories. Consequently, we examined the black start, set-point tracking, and load sharing performance of droop control, synchronverter and matching approach in a system-level simulation case study using IEEE 9-bus test system. Furthermore, a few conclusions regarding controllers tuning, their frequency time-scale and filtering impact have been drawn. Last but not least, we summarized the key challenges to be further investigated prior to large-scale GFC integration into low-inertia grids infrastructure.

REFERENCES

[1] B. Kroposki et al., “Achieving a 100% Renewable Grid: Operating Electric Power Systems with Extremely High Levels of Variable Renewable Energy,” IEEE Power and Energy Magazine, vol. 15, no. 2, pp. 61–73, Mar. 2017.

[2] G. Denis, T. Prevost, P. Panciatici, X. Kestelyn, F. Colas, and X. Guillaud, “Review on potential strategies for transmission grid operations based on power electronics interfaced voltage sources,” in 2015 IEEE Power Energy Society General Meeting, 2015, pp. 1–5.

[3] X. Wang, J. M. Guerrero, F. Blaabjerg, and Z. Chen, “A Review of Power Electronics Based Microgrids,” Journal of Power Electronics, vol. 12, no. 1, pp. 181–192, Jan. 2012.

[4] M.-S. Debry, G. Denis, T. Prevost, F. Xavier, and A. Menze, “Maximizing The Penetration Of Inverter-Based Generation On Large Transmission Systems: The Migrate Project,” presented at the 6th Solar Integration Workshop, 2016.

[5] M. C. Chandorkar, D. M. Divan, and R. Adapa, “Control of parallel connected inverters in standalone AC supply systems,” IEEE Transactions on Industry Applications, vol. 29, no. 1, pp. 136–143, Feb. 1993.

[6] Q.-C. Zhong and G. Weiss, “Synchronverters: Inverters That Mimic Synchronous Generators,” IEEE Transactions on Industrial Electronics, vol. 58, no. 4, pp. 1259–1267, Apr. 2011.

[7] Y. Chen, R. Hesse, D. Turschner, and H. P. Beck, “Dynamic properties of the virtual synchronous machine (VISMA),” Renewable Energy and Power Quality Journal, pp. 755–759, May 2011.

[8] Y. Han, H. Li, P. Shen, E. A. A. Coelho, and J. M. Guerrero, “Review of Active and Reactive Power Sharing Strategies in Hierarchical Controlled Microgrids,” IEEE Transactions on Power Electronics, vol. 32, no. 3, pp. 2427–2451, Mar. 2017.

[9] S. D’Arco and J. A. Suul, “Virtual synchronous machines #x2014; Classification of implementations and analysis of equivalence to droop controllers for microgrids,” in 2013 IEEE Grenoble Conference, 2013, pp. 1–7.

[10] H. Bevrani, T. Ise, and Y. Miura, “Virtual synchronous generators: A survey and new perspectives,” International Journal of Electrical Power & Energy Systems, vol. 54, no. Supplement C, pp. 244–254, Jan. 2014.

[11] T. Jouini, C. Arghir, and F. Dorfler, “Grid-forming Control for Power Converters based on Matching of Synchronous Machines,” arXiv:1706.09495 [math], Jun. 2017.

[12] S. Curi, D. Groß, and F. Dörfler, “Control of low-inertia power grids: A model reduction approach,” in 2017 IEEE 56th Annual Conference on Decision and Control (CDC), 2017, pp. 5708–5713.

[13] I. Cvetkovic, D. Boroyevich, R. Burgos, C. Li, and P. Mattavelli, “Modeling and control of grid-connected voltage-source converters emulating isotropic and anisotropic synchronous machines,” 2015, pp. 1–5.

[14] M. Sinha, F. Dorfler, B. B. Johnson, and S. V. Dhople, “Uncovering Droop Control Laws Embedded Within the Nonlinear Dynamics of Van der Pol Oscillators,” arXiv:1411.6973 [cs, math], Nov. 2014.

[15] B. B. Johnson, S. V. Dhople, J. L. Cale, A. O. Hamadeh, and P. T. Krein, “Oscillator-Based Inverter Control for Islanded Three-Phase Microgrids,” IEEE Journal of Photovoltaics, vol. 4, no. 1, pp. 387–395, Jan. 2014.

[16] B. Johnson, M. Rodriguez, M. Sinha, and S. Dhople, “Comparison of virtual oscillator and droop control,” 2017, pp. 1–6.

[17] M. Colombino, D. Groß, J.-S. Brouillon, and F. Dörfler, “Global phase and magnitude synchronization of coupled oscillators with application to the control of grid-forming power inverters,” arXiv:1710.00694 [math], Oct. 2017.

[18] A. Ortega, F. Miano, A. Musa, L. Toma, and D. Preotescu, “Definition of frequency under high dynamic conditions,” Technical report., deliverable 2.1, available at: www.re-serve.eu, 2017.

[19] A. H. Etemadi, E. J. Davison, and R. Iravani, “A Decentralized Robust Control Strategy for Multi-DER Microgrids #x2014;Part I: Fundamental Concepts,” *IEEE Transactions on Power Delivery*, vol. 27, no. 4, pp. 1843–1853, Oct. 2012.